# Electron-capture and ionization cross sections for collisions of $He^{2+}$ with Li: Production of $He^{+}(3l)$ at low velocities

E. J. Shipsey, L. T. Redmon, and J. C. Browne
*Department of Physics and Computer Sciences, University of Texas, Austin, Texas 78712*

R. E. Olson
*Molecular Physics Laboratory, SRI International, Menlo Park, California 94025*

(Received 3 March 1978)

Single-electron capture and ionization cross sections have been calculated for collisions of $He^{2+}$ with Li over the relative collision velocity range $0.1\text{–}10.0\times10^{8}$ cm/sec. For low collision velocities (i.e., $v = 0.1\text{–}0.6\times10^{8}$ cm/sec), a molecular approach has been used to determine the electron-capture cross section. *Ab initio* potential-energy curves and coupling matrix elements have been computed for the $(HeLi)^{2+}$ system and used in a cross-section evaluation based on the perturbed-stationary-state method. For the low velocities, the electron-capture reaction $He^{2+} + Li \rightarrow He^{+}(3l) + Li^{+}$ is found to dominate the collision process, and proceeds with a large cross section $\sigma \approx 10^{-15}$ cm$^2$, thus providing the possibility for population inversion and the subsequent emission of Lyman-$\alpha$ (304 Å) and Lyman-$\beta$ (256 Å) soft-x-ray photons. At the higher velocities (i.e., $v = 1.4\text{–}10.0\times10^{8}$ cm/sec), a classical-trajectory Monte Carlo method has been used to estimate both the electron-capture and ionization cross sections. At $2.2\times10^{8}$ cm/sec, both cross sections are found to be equal, while one ionization dominates the collisions process at higher velocities and electron-capture dominates at lower velocities.

## I. INTRODUCTION

The search for possible reactions that can give rise to vacuum ultraviolet (vuv) and x-ray radiation has recently centered on charge transfer reactions of multiply charged ions colliding with neutral species. The idea of using electron capture reactions was proposed by Vinogradov and Sobelman[1] and is based on the premise that collisions of the type

$$A^{+q} + B \rightarrow A^{+q-1} + B^{+} \tag{1}$$

preferentially leave the $A^{+q-1}$ product ion in a highly excited electronic state, which subsequently decays to its ground state with the emission of vuv or x-ray photons. Astrophysicists, Silk and Steigman,[2] have shown that reaction (1) with $B \equiv H$ and $A^{+q}$ a stripped metal ion, is a probable source for soft x rays in the interstellar medium. The experimental methods needed to utilize reaction (1) to make a superradiant or laser vuv or x-ray light source are very difficult and complex. However, Louisell *et al.*[3] and Anderson *et al.*[4] have proposed an experimental setup to make a soft x-ray laser based on reaction (1).

A fundamental issue in the use of reaction (1) to produce an x-ray laser is the specific choice of reactants. Consideration must also be given to the optimum collision velocity for producing a specific electronic level, the possible contamination of lower lying electronic levels that may preclude a population inversion, and whether or not the reaction can be realized experimentally.

One of the first restraints to consider is collision velocity. Generally, for high-velocity collisions ($v \gtrsim 2\times10^{8}$ cm/sec), the excitation of the $A^{+q-1}$ ion after electron capture tends to be spread over many electronic levels.[5] Thus, the cross section for producing a specific electronic state is small and the possibility of generating a population inversion is reduced. Also, the charge-transfer cross sections decrease rapidly with increasing collision velocity, even when the charge state of $A^{+q}$ is large.[6]

However, even if we restrict ourselves to low-velocity collisions, another restraint on the choice of collision partners must be acknowledged. For the more highly charged ions and many electron atomic targets, the reactant state lies in the continuum of the ionization + electron capture process

$$A^{+q} + B \rightarrow A^{+q-1} + B^{++} + e\,. \tag{2}$$

Hence, we may not only have electron capture to high lying states of $A^{+q-1}$ via (1), but also population of low-lying states of the $A^{+q-1}$ ion via reaction (2), thus removing the possibility of population inversion. Zwally and Koopman[7] very early recognized the importance of process (2) in the analysis of their $C^{+4} + Ar$ cross section data and, more recently, Winter *et al.*[8] have also shown reaction (2) to be an important process for collisions of multiply charged ions with many-electron targets such as Ne and Ar.

Cognizance of the above restraints on the choice of a specific collision system has led us to search for a reactant combination in which the target atom $B$ is light and the $A^{+q}$ ion is such that it will yield a specific $A^{+q-1}$ electronic level after collision. After

surveying many systems using semiempirical theoretical methods,[9,10] we were led to consider a more serious calculation on the $(HeLi)^{2+}$ system.

Our present calculations indicate that at low collision velocities ($v \lesssim 6\times10^7$ cm/sec), the electron capture reaction

$$He^{2+} + Li \rightarrow He^{+} + Li^{+} \tag{3}$$

preferentially produces excited $He^+(3l)$, which will decay either directly to its ground state with the emission of a 256-Å (48.4 eV) photon or by cascading via the $He^+(2l)$ level with the emission of 1640-Å (7.6 eV) and 304-Å (40.8 eV) photons.

Potential energy curves and cross sections for reaction (3) are presented below. We have used two theoretical methods—a molecular approach for low-velocity collisions and a classical-trajectory Monte-Carlo method for high-velocity collisions—in order to predict the cross sections for electron capture, reaction (3), and ionization

$$He^{2+} + Li \rightarrow He^{2+} + Li^{+} + e \tag{4}$$

over the range of velocities $v=(0.1-10.0)\times10^8$ cm/sec.

## II. MOLECULAR WAVE FUNCTIONS AND ORBITALS

The molecular wave functions used as the adiabatic basis are of the generalized valence-bond configuration-interaction type. A full description of the characteristics of these wave functions can be found in Matsen and Browne.[11,12] This basis is particularly well suited to this collision problem since highly excited states are readily representable.

The wave functions for the doublet sigma and pi states are given in Tables I and II. Each term represents a Slater determinant consisting of Slater orbitals. The coefficients of minus $r$ in the exponential term of the Slater orbital are given in Tables III and IV. The orbitals enclosed in parentheses are spin-paired.

There are three charge configurations to account for in the system: $LiHe^{2+}$, $Li^+He^+$, and $Li^{2+}He$. The first 12 terms of $\Psi_\Sigma$ and the first 6 terms of $\Psi_\Pi$ correspond to $LiHe^{2+}$. Terms 13 through 21 of $\Psi_\Sigma$ and terms 7 through 10 of $\Psi_\Pi$ correspond to $Li^+He^+$. Finally, the last 7 terms of $\Psi_\Sigma$ and the last 2 terms of $\Psi_\Pi$ account for $Li^{2+}He$.

An attempt has been made to achieve the proper spacing of the energy levels in the three systems. "Correlation" terms of the type $(1s\,1s')$ and $(2p)^2$ have been included to lower the energy of the more correlated terms of the separated subsystems. To account for the polarizabilities of the separated subsystems, we have included orbitals that represent $z$ times some of the more important atomic orbitals.

The matrix elements which couple the adiabatic states of the molecular representation are due to the relative velocity of the collision pair. The two significant operators[13] are $\partial/\partial R$ which represents motion along the internuclear line and $L_x$ which is the rotational component. The $\partial/\partial R$ operator introduces $\Sigma$-$\Sigma$ coupling while the $L_x$ operator introduces $\Sigma$-$\Pi$ coupling. A brief description of the computational processes for the matrix elements can be found in Olson, Shipsey, and Browne.[14]

The computation of the wave function and coupling matrix elements were carried out with the standard computer programs of the Molecular Physics Group at the University of Texas.

The potential energy curves obtained from our calculations are shown in Fig. 1. We should note that the molecular state $\Sigma_4$ correlating to the $He^{2+}+Li$ system crosses the $He^+(3l)+Li^+$ manifold at $R$ values ranging from $(33-44)\,a_0$. We have performed self-consistent field (SCF) calculations to investigate this outer crossing region and are able to conclude that at the collision velocities of interest here, the particles proceed diabatically onto the $\Sigma_4$ state. Only for thermal energy collisions

TABLE I. $\Sigma$ wave function.

$$\begin{aligned}
\Psi_\Sigma = {} & A_1(1s_{Li})^2 2s_{Li} + A_2(1s_{Li})^2 3s_{Li} + A_3(1s_{Li})^2 4s_{Li} + A_4(2p^0_{Li})^2 2s_{Li} \\
& + A_5(2p^-_{Li}2p^+_{Li})2s_{Li} + A_6(1s_{Li})^2 3p^0_{Li} + A_7(1s_{Li})^2 4p^0_{Li} + A_8(1s_{Li})^2 5p^0_{Li} \\
& + A_9(2p^0_{Li})^2 3p^0_{Li} + A_{10}(2p^-_{Li}2p^+_{Li})3p^0_{Li} + A_{11}(1s_{Li}2p^{0'}_{Li})2s_{Li} + A_{12}(1s_{Li})^2 2p^{0''}_{Li} \\
& + A_{13}(1s'_{Li}1s''_{Li})1s_{He} + A_{14}(1s'_{Li}1s''_{Li})1s'_{He} + A_{15}(1s'_{Li}1s''_{Li})2s_{He} \\
& + A_{16}(1s'_{Li}1s''_{Li})2p^0_{He} + A_{17}(1s'_{Li}1s''_{Li})3s_{He} + A_{18}(1s'_{Li}1s''_{Li})3p^0_{He} \\
& + A_{19}(1s'_{Li}1s''_{Li})3d^0_{He} + A_{20}(1s'_{Li}1s''_{Li})4s_{He} + A_{21}(1s'_{Li}1s''_{Li})4p^0_{He} \\
& + A_{22}(1s''_{He}1s'''_{He})1s'''_{Li} + A_{23}(1s''_{He}2p^{0''}_{He})1s'''_{Li} + A_{24}(1s'''_{He}2p^{0'}_{He})1s'''_{Li} \\
& + A_{25}(1s_{He}2p^{0'''}_{He})1s'''_{Li} + A_{26}(1s_{He}2s_{He})1s'''_{Li} + A_{27}(1s_{He}1s'''_{Li})2p^{0'''}_{He} \\
& + A_{28}(1s_{He}1s'''_{Li})2s_{He}
\end{aligned}$$

TABLE II. Π wave function.

$$\Psi_{\Pi} = B_1(1s_{Li})^2 3p^+_{Li} + B_2(1s_{Li})^2 4p^+_{Li} + B_3(2p^0_{Li})^2 3p^+_{Li} + B_4(2p^-_{Li}2p^+_{Li})3p^+_{Li} + B_5(1s_{Li}2p^{+\prime}_{Li})2s_{Li} + B_6(1s_{Li})^2 2p^{+\prime\prime}_{Li} + B_7(1s'_{Li}1s''_{Li})2p^+_{He} + B_8(1s'_{Li}1s''_{Li})3p^+_{He} + B_9(1s'_{Li}1s''_{Li})3d^+_{He} + B_{10}(1s'_{Li}1s''_{Li})4p^+_{He} + B_{11}(1s_{He}2p^{+\prime}_{He})1s'''_{Li} + B_{12}(1s_{He}1s'''_{Li})2p^{+\prime}_{He}$$

will an electron capture cross section of $\sim 10^{-15}$ cm$^2$ result from the long range interactions, the products being $He^+(3l) + Li^+$.

There is an avoided crossing between the $\Sigma_4$ and $\Sigma_5$ states at $R \approx 5.5a_0$. Landau-Zener calculations indicate that the probability that the particles will follow the diabatic potential ($\Sigma_4$ for $R > 5.5a_0$ and $\Sigma_5$ for $R < 5.5a_0$) is close to unity. Hence, for our low velocity cross section evaluation we need to be concerned only with the interactions between $\Sigma_4$ for $R > 5.5a_0$ and $\Sigma_5$ for $R < 5.5a_0$ with other close-lying Σ and Π states. From the computed $L_x$ rotational coupling matrix elements and the $\partial/\partial R$ radial coupling matrix elements, we are able to conclude there is only one significant interaction: rotational coupling to the $\Pi_2$ state whose separated atom products are $He^+(3p)$ and $Li^+$. The reactions leading to products other than $He^+(3l)$ thus should, at appreciable collision velocities, have cross-sections very much smaller than those leading to $He^+(3l)$. The computed rotational coupling matrix elements and the potential energy differences between the $\Sigma_4$-$\Pi_2$ and $\Sigma_5$-$\Pi_2$ states are given in Fig. 2. We should caution that although the electron

TABLE III. Σ orbitals.

| Orbital | Exponent | Orbital | Exponent |
|---|---|---|---|
| $1s_{Li}$ | 2.6864 | $1s_{He}$ | 2.0000 |
| $1s'_{Li}$ | 3.2949 | $1s'_{He}$ | 1.0000 |
| $1s''_{Li}$ | 2.0790 | $1s''_{He}$ | 2.1832 |
| $1s'''_{Li}$ | 3.0000 | $1s'''_{He}$ | 1.1885 |
| $2s_{Li}$ | 0.6374 | $2s_{He}$ | |
| $2p^-_{Li}$ | | $2p^0_{He}$ | 1.0000 |
| $2p^0_{Li}$ | 3.9756 | $2p^{0\prime}_{He}$ | 2.1832 |
| $2p^+_{Li}$ | | $2p^{0\prime\prime}_{He}$ | 1.1885 |
| $2p^{0\prime}_{Li}$ | 2.6864 | $2p^{0\prime\prime\prime}_{He}$ | 0.4868 |
| $2p^{0\prime\prime}_{Li}$ | 0.5256 | $3s_{He}$ | |
| $3s_{Li}$ | 0.9563 | $3p^0_{He}$ | 0.6667 |
| $3p^0_{Li}$ | 0.6374 | $3d^0_{He}$ | |
| $4s_{Li}$ | | $4s_{He}$ | 0.7183 |
| $4p^0_{Li}$ | 0.9563 | $4p^0_{He}$ | 0.7285 |
| $5p^0_{Li}$ | | | |

TABLE IV. Π orbitals.

| Orbital | Exponent | Orbital | Exponent |
|---|---|---|---|
| $1s_{Li}$ | 2.6864 | $1s_{He}$ | 2.0000 |
| $1s'_{Li}$ | 3.2949 | $2p^+_{He}$ | 1.0000 |
| $1s''_{Li}$ | 2.0790 | $2p^{+\prime}_{He}$ | 0.4868 |
| $1s'''_{Li}$ | 3.0000 | $3p^+_{He}$ | 0.6667 |
| $2s_{Li}$ | 0.6374 | $3d^+_{He}$ | 0.6667 |
| $2p^-_{Li}$ | | $4p^+_{He}$ | 0.7285 |
| $2p^0_{Li}$ | 4.0144 | | |
| $2p^+_{Li}$ | | | |
| $2p^{+\prime}_{Li}$ | 2.6864 | | |
| $2p^{+\prime\prime}_{Li}$ | 0.5256 | | |
| $3p^+_{Li}$ | 0.6374 | | |
| $4p^+_{Li}$ | 0.9667 | | |

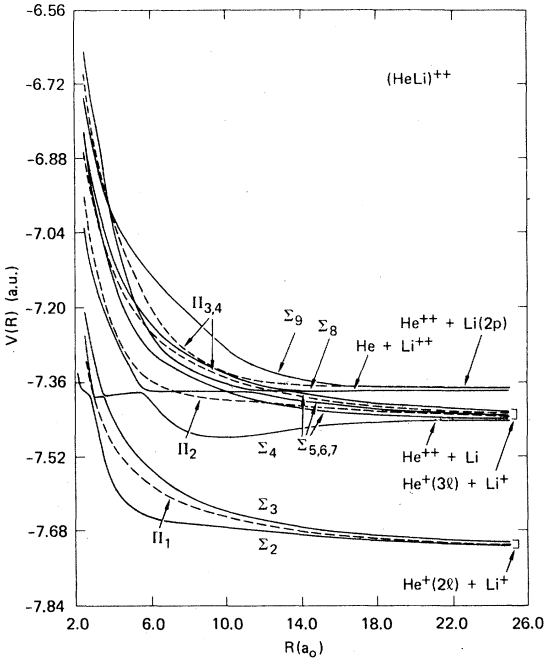


FIG. 1. Potential energy curves for the $(HeLi)^{2+}$ system. Solid lines denote $^2\Sigma$ molecular states; dashed lines denote $^2\pi$ molecular states. Note the diabatic potential curves that correlate to the $He^{2+}$ + Li reactants, $\Sigma_5$ for $R \lesssim 6.0\ a_0$ and $\Sigma_4$ for $R \gtrsim 6.0\ a_0$. These states are coupled strongly via rotational coupling to the $\pi_2$ state which dissociates to $He^+(3p)$ + $Li^+$.

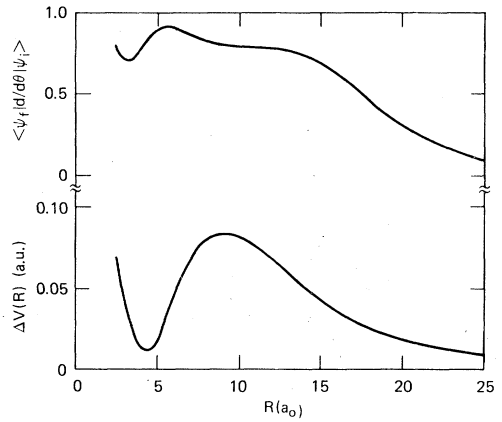


FIG. 2. Rotational coupling matrix element and potential energy difference between the $\pi_2$ state of $He^+(3p)+Li^+$ and the $\Sigma_5$ (for $R \lesssim 6.0a_0$) and $\Sigma_4$ ($R \gtrsim 6.0\ a_0$) states which correlated diabatically to the $He^{2+}+Li$ reactants.

capture proceeds to a state correlating to $He^+(3p)+Li^+$, long range interactions between all the states arising from $He^+(3l)+Li^+$ will considerably distort the product distribution. At this time, we are unable to predict the specific product distribution among the $3s$, $3p$, and $3d$ levels of $He^+$.

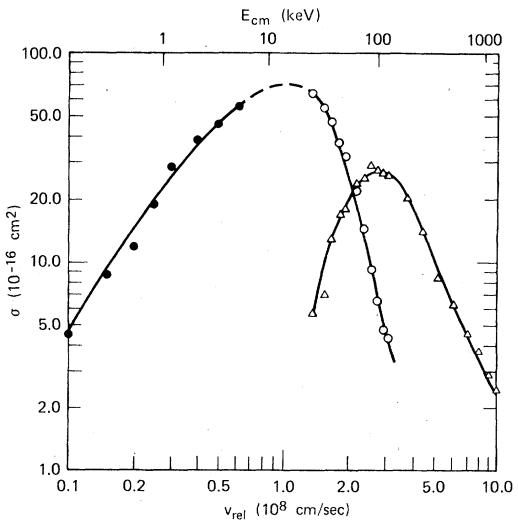


FIG. 3. Calculated electron-capture cross section for reaction (3) using a molecular approach that is appropriate for low-velocity collisions, solid circles, and a classical-trajectory Monte-Carlo approach that is valid for high velocity collisions, open circles. The ionization cross section for reaction (4) calculated using the classical-trajectory Monte-Carlo method is shown by the open triangles.

## III. CROSS-SECTION EVALUATION

### A. Low collision velocities

The low-velocity electron capture cross section evaluations were carried out using the perturbed-stationary-state approximation.[15] In this approximation, the particles follow straight-line classical trajectories while the electronic transitions are treated quantum mechanically. Because of the nature of the $(LiHe)^{2+}$ interactions, it is necessary to solve only two coupled equations of the general form:

$$\frac{dc_i(\zeta)}{d\zeta} = -\sum_j \Gamma_{ij}(\zeta)\exp[-i\omega_{ij}(\zeta)]\,c_j(\zeta)\,. \tag{5}$$

In Eq. (5), $\zeta$ is related to the impact parameter $b$ and the internuclear separation $R$ by $\zeta^2 = R^2 - b^2$. The interaction potentials $V_i$ arise in (5) as differences via

$$\omega_{ij}(\zeta) = \frac{1}{\hbar v}\int_{-\infty}^{\zeta}(V_j - V_i)\,d\zeta'\,, \tag{6}$$

while the matrix elements for rotational coupling are given by

$$\Gamma_{ij} = (b/R)\,L_{ij}\,. \tag{7}$$

The total cross section for a transition from channel $i$ to channel $j$ is then given by

$$Q_j = 2\pi\int_0^{\infty} db\,b\,|c_j|^2\,. \tag{8}$$

Figure 2 gives the necessary potential difference and rotational coupling matrix element information needed for the cross-section evaluation for the electron capture reaction

$$He^{2+}+Li \rightarrow He^+(3l)+Li^+\,. \tag{9}$$

In Fig. 3 the cross sections for reaction (9) obtained by solving Eqs. (5)–(8) are shown by solid circles. The cross sections rise with increasing velocity and are large, $\sigma \approx 10^{-15}$ cm$^2$.

Since we have not included electron translational factors in the cross section evaluations, it is not valid to extend the calculations to collision velocities comparable to the orbital velocity $v_e$ of the electron being captured. Hence, for reaction (9) we have restricted our calculations to collision velocities $v \lesssim \frac{1}{2}v_e$, where for a Li atom target, $v_e \simeq 1.4\times10^8$ cm/sec.

As a rough estimate of the cross-section sensitivity, we have varied the potential differences given in Fig. 2 by ±50% and have recalculated the cross sections. The cross sections changed by +60% and −40%, almost linearly with the potential difference change. We have also investigated the effect of changing the origin for the coupling matrix element evaluation from the center of mass to ori-

gins on the Li or He nucleus. The cross sections varied only slightly with these changes, less than ±10%, and hence may be considered insignificant. Given the probable accuracy of the potential curves relative to one another, our estimate of the cross section accuracy is approximately ±50%. However, we do not expect the collision mechanism, that is, production of $He^+(3l)$, to be changed by reasonable variations in the potential curves.

### B. High collision velocities

For the high-velocity collisions, we have used a classical-trajectory Monte-Carlo method that has been previously described in detail.[16] This theoretical method is based on solving Hamilton's equations of motion for a three-particle system.[17] Basic to the successful application of the method to interactions between charged projectiles and a hydrogenic target is the classical description of the target atom developed by Abrines and Percival.[18] Percival and Richards[19] have previously argued that the classical-trajectory method will be valid for collision velocities $v \gtrsim v_e$, which for a Li atom target corresponds to $v \gtrsim 1.4\times10^8$ cm/sec.

The classical-trajectory method has been successful in predicting the electron capture and ionization cross sections for collisions of multiply-charged ions and atomic hydrogen targets.[16] For our application to the $(LiHe)^{2+}$ system and reactions (3) and (4), it is necessary to describe the Li atom target as an active electron and a point charge for the $Li^+$ nucleus. We have taken 5.39 eV (the ionization potential for Li) as the energy for the orbital electron and 1.3 as the charge for the $Li^+$ nucleus. The value of 1.3 is consistent with Slater's rules[20] for the nuclear charge seen by the Li valence electron and is very close to the value of 1.28 obtained by Clementi and Roetti[21] in their optimization of a single zeta basis set for Li.

The results of classical-trajectory Monte-Carlo calculations are displayed by open symbols in Fig. 3. Electron capture dominates the collision process at velocities $v \lesssim 2.2\times10^8$ cm/sec, whereas the ionization process dominates at the higher velocities. At the highest velocities we have also investigated the possibility of electron capture or ionization out of the core of the Li atom. No significant contribution was obtained.

As mentioned in the Introduction, the electron capture cross section generally decreases precipitately with increasing velocity when $v \gtrsim 2\times10^8$ cm/sec, as shown in Fig. 3. Also, at the higher velocities the electron capture proceeds into a band of electronic levels that broadens with increasing velocity, thus removing the selectivity of the excited electronic states produced. In the classical-trajectory calculations we have monitored this latter behavior by tabulating the energy of the captured electron after collision. At a collision velocity of $1.4\times10^8$ cm/sec, we find 7% of the electrons are captured in the $n=1$ state of $He^+$, 46% in $n=2$, 23% in $n=3$, 10% in $n=4$, and 6% in $n=5$. With an increase in the collision velocity to $2.2\times10^8$ cm/sec, this distribution broadens to 7% in $n=1$, 27% in $n=2$, 19% in $n=3$, 13% in $n=4$, and 10% in $n=5$. Hence, at collision velocities $v \gtrsim v_e$, it appears that it will be difficult to realize a population inversion, even though high-lying electronic levels of the ion are produced.

## IV. CONCLUDING REMARKS

Electron capture and ionization cross sections have been calculated for the $He^{2+}+Li$ system over a wide range of collision velocities, $v = 0.1 - 10.0 \times 10^8$ cm/sec. At low velocities, $v \lesssim 6\times10^7$ cm/sec, the calculations indicate $He^+(3l)$ will be selectively produced during the collision. Thus, it appears the $He^{2+}+Li$ system will very efficiently produce soft x-ray photons at wavelengths 256 Å and 304 Å.

The optimum conditions under which a population inversion could be attained are also discussed. It appears that low velocity $v < v_e$ collisions will be most efficient in this regard, at higher energies the product state distributions tend to broaden considerably and also the cross section for electron capture decreases rapidly with increasing velocity. It should be noted, however, that in low velocity collisions between multiply charged ions and many electron target atoms, the ionization + electron capture process, reaction (2), will be very important. This process tends to leave the product $A^{+q-1}$ ion in a low-lying excited or ground state, thereby removing the possibility for population inversion.

## ACKNOWLEDGMENTS

The authors (E.J.S., L.T.R., and J.C.B.) acknowledge support from the Office of Naval Research under Contract No. N00014-67-A-0126-017 and from the Welch Foundation under Grant No. F-379, whereas R.E.O. acknowledges support by SRI internal research and development funds.

[1]A. V. Vinogradov and I. I. Sobelman, Zh. Eksp. Teor. Fiz. 63, 2113 (1972) [Sov. Phys. JETP 36, 115 (1973)].
[2]J. Silk and G. Steigman, Phys. Rev. Lett. 23, 597 (1969).
[3]W. H. Louisell, M. O. Scully, and W. B. McKnight, Phys. Rev. A 11, 989 (1975).
[4]D. Anderson, J. McCullen, M. O. Scully, and J. F. Seely, Opt. Commun. 17, 226 (1976).
[5]J. A. Guffey, L. D. Ellsworth, and J. R. MacDonald, Phys. Rev. A 15, 1863 (1977).
[6]K. H. Berkner, W. G. Graham, R. V. Pyle, A. S. Schlachter, J. W. Stearns, and R. E. Olson, J. Phys. B (to be published).
[7]H. J. Zwally and D. W. Koopman, Phys. Rev. A 2, 1851 (1970).
[8]H. Winter, E. Bloemen, and F. J. DeHeer, J. Phys. B 10, L599 (1977).
[9]R. E. Olson, F. T. Smith, and E. Bauer, Appl. Opt. 10, 1848 (1971).
[10]R. E. Olson and A. Salop, Phys. Rev. A 14, 579 (1976).
[11]F. A. Matsen and J. C. Browne, J. Phys. Chem. 66, 2332 (1962).
[12]F. A. Matsen and J. C. Browne, Phys. Rev. A 135, 1227 (1964).
[13]D. R. Bates, H. S. W. Massey, and A. L. Stewart, Proc. R. Soc. London Ser. A 216, 437 (1953).
[14]R. E. Olson, E. J. Shipsey, and J. C. Browne, J. Phys. B 11, 699 (1978).
[15]D. R. Bates and R. MacCarroll, Proc. R. Soc. London Ser. A 245, 175 (1958).
[16]R. E. Olson and A. Salop, Phys. Rev. A 16, 531 (1977).
[17]M. Karplus, R. N. Porter, and R. D. Sharma, J. Chem. Phys. 43, 3259 (1965).
[18]R. Abrines and I. C. Percival, J. Phys. B 88, 861 (1966).
[19]I. C. Percival and D. Richards, *Advances in Atomic and Molecular Physics*, edited by D. R. Bates and I. Esterman (Academic, New York, 1975), Vol. II, p. 1.
[20]H. Eyring, J. Walter, and G. E. Kimball, *Quantum Chemistry* (Wiley, New York, 1964), p. 162.
[21]E. Clementi and C. Roetti, At. Data Nucl. Data Tables 14, 177 (1974).